Journal of Neurochemistry, 2003, **86**, 1101–1107 doi:10.1046/j.1471-4159.2003.01908.x

Regulation of brain mitochondrial H_2O_2 production by membrane potential and NAD(P)H redox state

Anatoly A. Starkov and Gary Fiskum

Department of Anesthesiology, University of Maryland School of Medicine, Baltimore, Maryland, USA

Abstract

Mitochondrial production of reactive oxygen species (ROS) at Complex I of the electron transport chain is implicated in the etiology of neural cell death in acute and chronic neurodegenerative disorders. However, little is known regarding the regulation of mitochondrial ROS production by NADH-linked respiratory substrates under physiologically realistic conditions in the absence of respiratory chain inhibitors. This study used Amplex Red fluorescence measurements of H_2O_2 to test the hypothesis that ROS production by isolated brain mitochondria is regulated by membrane potential ($\Delta\Psi$) and NAD(P)H redox state. $\Delta\Psi$ was monitored by following the medium concentration of the lipophilic cation tetraphenylphosphonium with a selective electrode. NAD(P)H autofluorescence was used to monitor NAD(P)H redox state. While the rate of H_2O_2 production was closely related to $\Delta\Psi$ and the level of NAD(P)H reduction at high values of $\Delta\Psi$, 30% of the maximal rate of H_2O_2 formation was still observed in the presence of uncoupler (*p*-trifluoromethoxycarbonylcyanide phenylhydrazone) concentrations that provided for maximum depolarization of $\Delta\Psi$ and oxidation of NAD(P)H. Our findings indicate that ROS production by mitochondria oxidizing physiological NADH-dependent substrates is regulated by $\Delta\Psi$ and by the NAD(P)H redox state over ranges consistent with those that exist at different levels of cellular energy demand.

Keywords: brain mitochondria, hydrogen peroxide, membrane potential, reactive oxygen species.

J. Neurochem. (2003) **86,** 1101–1107.

Mitochondrial production of reactive oxygen species (ROS) is involved in neural cell death associated with acute ischemic brain injury and with chronic neurodegenerative diseases (Fiskum 2000; Nicholls and Budd 2000). Several potential sites of ROS production exist within the mitochondrial electron transport chain. Recent attention has focused on respiratory chain Complex I as an important source of free radicals, due in part to the stimulation of ROS production and induction of oxidative stress caused by neurotoxins, e.g. 1-methyl-4-phenylpyridinium (MPP^+) and rotenone, that target Complex I and evoke a neuropathology similar to that of Parkinson's disease (Sherer *et al*. 2002). The molecular mechanism and regulation of ROS production by Complex I is, however, not well understood (reviewed in Turrens 1997).

As Complex I may be a primary site of mitochondrial ROS generation in the absence of toxins as well as in their presence, identification of physiological factors that control Complex I mediated ROS production is necessary. We hypothesized that such factors include mitochondrial membrane potential and NAD(P)H redox state. Both undergo substantial fluctuation in response to different levels of mitochondrial respiratory activity caused by, for example, different demand for ATP production. Modulation of these factors by the activities of mitochondrial uncoupling proteins and by the mitochondrial ATP-regulated potassium channel may also explain their apparent ability to reduce mitochondrial ROS production (Kim-Han *et al*. 2001; Echtay *et al*. 2002; Ferranti *et al*. 2003). The results of this study support the hypothesis that biologically relevant, NADH linked substrate-dependent mitochondrial ROS production is tightly controlled by membrane potential and NAD(P)H redox state in the physiological range.

Resubmitted manuscript received March 23, 2003; accepted April 29, 2003.

Address correspondence and reprint requests to Dr Gary Fiskum, Department of Anesthesiology, University of Maryland School of Medicine, 685 W. Baltimore St., MSTF-5.34, Baltimore, MD 21201, USA. E-mail: gfisk001@umaryland.edu

Abbreviations used: ACI, acceptor control index; $\Delta\Psi$, mitochondrial membrane potential; FCCP, *p*-trifluoromethoxycarbonylcyanide phenylhydrazone, MPP^+, 1-methyl-4-phenylpyridinium; ROS, reactive oxygen species; TPP^+, tetraphenylphosphonium.

Materials and methods

Isolation of brain mitochondria

All animal experiments were conducted in accordance with guidelines established by the Institutional Animal Care and Use Committee of the University of Maryland, Baltimore.

Brain mitochondria were isolated from adult male Sprague Dawley rats as described in Rosenthal *et al*. (1987), with the only modification that our isolation buffer did not contain Nagarse protease. This method utilizes digitonin to disrupt synaptosomal membranes, yielding mitochondria from both synaptosomal and non-synaptosomal origin. The functional quality of each mitochondrial preparation was estimated by measuring acceptor control index (ACI). For these experiments, incubation medium was composed of 125 mM KCl, 20 mM HEPES (pH 7.0), 2 mM KH_2PO_4, 0.8 mM ADP, 1 mM $MgCl_2$, 5 mM glutamate, and 5 mM malate. Oxygen consumption was recorded with a Clark-type oxygen electrode. The State 3 respiration was initiated by the addition of 0.5 mg/mL rat brain mitochondria to the incubation medium, and was terminated with 0.5 μg/mL oligomycin. The ratio of respiration rate in State 3 to that in the presence of oligomycin was defined as ACI. Preparations exhibiting values for ACI in the range of 8–12 were used for this study.

Experimental conditions and incubation medium

Incubation medium contained 125 mM KCl, 20 mM HEPES (pH 7.0), 2 mM KH_2PO_4, 1 mM $MgCl_2$, 0.5 mg/mL bovine serum albumin, and 0.25 mM EGTA, and was maintained at 37°C, unless stated otherwise.

Measurement of hydrogen peroxide

Hydrogen peroxide production was measured fluorimetrically employing the dye Amplex Red (Molecular Probes, Eugene, OR, USA) in combination with horseradish peroxidase (Kushnareva *et al*. 2002; Rosen *et al*. 2002). In these experiments, the incubation medium was supplemented with 1 μM amplex red, 5 U/mL horseradish peroxidase, and 40 U/mL Cu,Zn superoxide dismutase. The presence of superoxide dismutase prevents the auto-oxidation of Amplex Red that interferes with quantitative assessment of low rates of H_2O_2 production. The detection of H_2O_2 in mitochondrial suspensions was recorded as an increase in fluorescence of the dye at 585 nm with the excitation wavelength set at 550 nm. The dye response was calibrated either by sequential additions of known amounts of hydrogen peroxide solution, or by continuous infusion of H_2O_2 solution at 100–1000 pmol/min. The concentration of commercial 30% H_2O_2 solution was calculated from light absorbance at 240 nM employing $E^{240} = 43.6\ \text{M}^{-1}\ \text{cm}^{-1}$; the stock solution was diluted to 100 μM with de-ionized water and used for calibration immediately.

Measurement of mitochondrial membrane potential

Mitochondrial membrane potential ($\Delta\Psi$) was estimated from tetraphenylphosphonium (TPP^+) ion distribution measured with a custom-made TPP^+-selective electrode (Kamo *et al*. 1979). For these experiments, incubation medium was supplemented with 1.6 μM TPP^+Cl^-. Both the TPP^+-sensitive and the reference electrodes were inserted directly into the fluorimeter cuvette and data were collected using an amplifier and a two-channel data acquisition system. The electrode response was calibrated by sequential additions of TPP^+Cl^- in the range of concentrations 0.2–1.6 μM and $\Delta\Psi$ was calculated as described in Rolfe *et al*. (1994) utilizing the reported binding correction factor for brain mitochondria. Alternatively, $\Delta\Psi$ values were calculated by the procedure reported in Rottenberg (1984), assuming the matrix volume for brain mitochondria equal to 1.2 μL/mg protein. Both procedures gave essentially similar results. No attempt to correct for non-$\Delta\Psi$ dependent binding of TPP^+ was made (Hashimoto *et al*. 1984; Rottenberg 1984; Rolfe *et al*. 1994).

Measurement of NAD(P)H oxidation/reduction state

Reduced NAD(P)H was measured fluorimetrically using an excitation wavelength of 346 nm and an emission wavelength of 460 nm. Maximal NAD(P)H reduction was defined as the absorbance observed after the addition of the electron transport chain Complex I inhibitor rotenone (1 μM) and maximal oxidation defined as the absorbance obtained in the presence of the respiratory uncoupler *p*-trifluoromethoxycarbonylcyanide phenylhydrazone (FCCP) (0.1 μM).

Reagents

Oligomycin, FCCP, and rotenone were dissolved in ethanol, and Amplex Red was dissolved in dimethylsulfoxide. All reagents and ethanol were tested and exhibited no interference with H_2O_2 assay at the concentrations used in our experiments. All the reagents were purchased from Sigma (St Louis, MO, USA).

Results

The results shown in Fig. 1 illustrate the dependence of H_2O_2 production on mitochondrial $\Delta\Psi$ in the presence of NADH-linked respiratory substrates. Suspensions of rat brain mitochondria were exposed to various concentrations (0–80 nM) of the uncoupler FCCP to lower $\Delta\Psi$. Alternatively, mitochondria were exposed to ADP (0.8 mM) to reduce $\Delta\Psi$ as a consequence of activating State 3 respiration, i.e. oxidative phosphorylation. H_2O_2 production was measured fluorimetrically with the dye Amplex Red and $\Delta\Psi$ was calculated based on the medium/mitochondrial distribution of the lipophilic cation TPP^+, as measured with an electrode placed within the fluorometer cuvette. Malate plus glutamate or α-ketoglutarate were used as NADH-linked substrates.

In the presence of either set of NADH-linked oxidizable substrates, a reduction in $\Delta\Psi$ was accompanied by a decrease in H_2O_2 production (Fig. 1). This relationship between H_2O_2 production and $\Delta\Psi$ is qualitatively similar to that reported earlier for heart mitochondria oxidizing the Complex II respiratory substrate succinate (Korshunov *et al*. 1997). However, whereas a small, 10% reduction in $\Delta\Psi$ resulted in a 90% reduction in succinate-supported ROS production (Korshunov *et al*. 1997), approximately 30% of the maximal rate of NADH-linked substrate dependent ROS production was still present at a concentration of FCCP that caused maximal reduction of membrane potential (Fig. 1) and a maximal increase in O_2 consumption (not shown). Addition

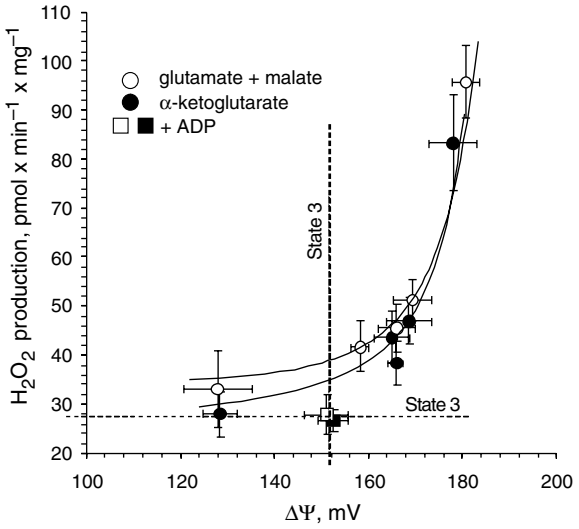

Fig. 1 Relationship between mitochondrial membrane potential and H_2O_2 production supported by NADH-linked respiratory substrates. Mitochondrial membrane potential was calculated based on the distribution of the lipophilic cation TPP^+, using an electrode to measure the medium [TPP^+] (1.2 μM initial concentration). H_2O_2 was measured simultaneously by monitoring the fluorescence of Amplex Red (1 μM) in the presence of horseradish peroxidase (5 U/mL) and 40 U/mL Cu/Zn superoxide dismutase. Incubation medium (see 'Materials and methods') maintained at 37°C also contained either 5 mM malate + 5 mM glutamate (○) or 5 mM α-ketoglutarate (●). Mitochondria were added at 0.5 mg/mL. Differences in membrane potential were generated by adding various concentrations of FCCP ranging from 0 to 80 nM (0–160 pmol/mg mitochondrial protein). Alternatively, a decrease in membrane potential was induced by adding 0.8 mM ADP to mitochondria respiring on malate + glutamate (□) or α-ketoglutarate (■). Values represent means ± SD for $n = 4$ experiments.

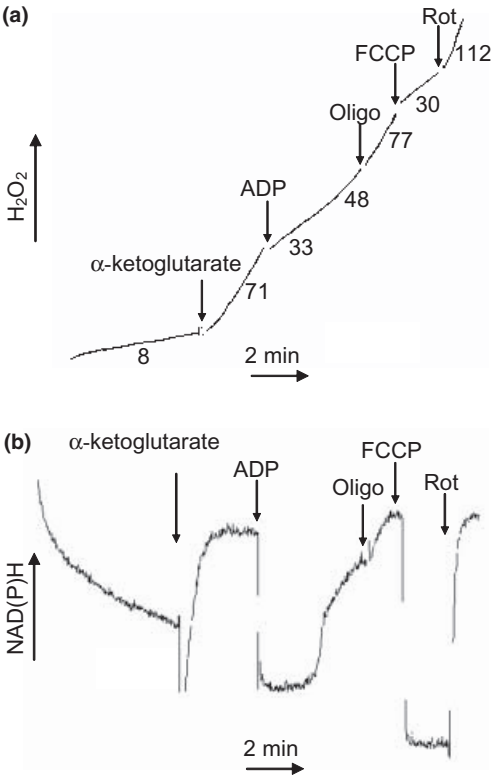

Fig. 2 Regulation of mitochondrial H_2O_2 production through metabolic modulation of NAD(P)H redox state. (a) H_2O_2 production by brain mitochondria. (b) Mitochondrial NAD(P)H autofluorescence. Incubation medium (see 'Materials and methods') maintained at 37°C was supplemented with 5 U/mL horseradish peroxidase, 1 μM Amplex red, and 40 U/mL SOD. Mitochondria were added at 0.5 mg/mL. Additions to the suspensions were α-ketoglutarate (5 mM), ADP (0.8 mM), oligomycin (0.5 μg/ml), FCCP (80 nM), and rotenone (0.5 μM).

of even greater FCCP concentrations had no further effect on either ROS production or TPP^+ distribution. As the TPP^+ procedure for monitoring ΔΨ is incapable of detecting potentials at less than approximately 120 mV, these observations indicate that a significant fraction of maximal NADH-dependent mitochondrial ROS production can occur in the absence of ΔΨ.

A 70% reduction in ROS generation was also observed in the absence of FCCP when ADP was added to initiate oxidative phosphorylation, thereby stimulating respiration (Fig. 1). Therefore, physiologically relevant NADH-linked respiration generates ROS in a manner that is tightly regulated by differences in ΔΨ over a range that occurs during normal fluctuations in energy metabolism. The approximately 70% reduction in ROS production during State 3 respiration was, however, observed at a level of ΔΨ that was approximately 20 mV greater than that present at the same rate of ROS generation evoked by the addition of FCCP.

The redox state of mitochondrial pyridine nucleotides is sensitive to changes in ΔΨ when respiration is supported by NADH-linked substrates. We therefore performed parallel measurements of H_2O_2 production and reduced NAD(P)H to determine their relationship (Fig. 2). Addition of brain mitochondria to medium in the absence of respiratory substrates resulted in a steady oxidized shift of pyridine nucleotides and a relatively very low rate of H_2O_2 production. In the absence of exogenous oxidizable substrates, respiration is also minimal. Thus the flow of electrons limits both ROS production and O_2 consumption under these conditions. Addition of the respiratory substrate α-ketoglutarate caused an abrupt increase in the level of reduced NAD(P)H and stimulated ROS production by almost 10-fold. Subsequent addition of 0.8 mM ADP resulted in an immediate and extensive oxidation of pyridine nucleotides and a > 50% reduction in H_2O_2 production. During the next 4 min, the pyridine nucleotide redox state underwent a partial reversal toward reduction, accompanied by an increase in ROS production. Independent measurements of O_2 consumption verify that this transition is due to the deceleration of State 3 respiration toward resting, State 4 respiration (data

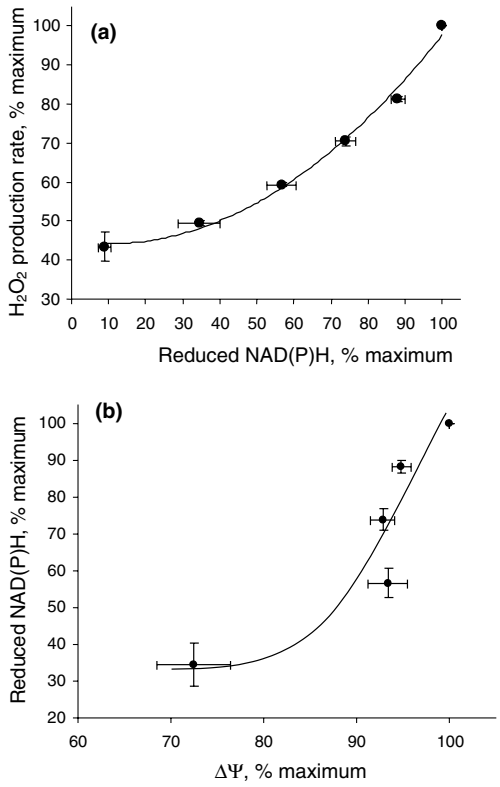

Fig. 3 Relationships between mitochondrial H_2O_2 production, NAD(P)H redox state, and membrane potential. Mitochondrial H_2O_2 production (a), NAD(P)H redox state (b), and membrane potential (b) were measured as described for Figs 1 and 2 in the presence of glutamate + malate and the uncoupler FCCP at concentrations of from 0 to 80 nM. Values represent means ± SD obtained from $n = 4$ experiments and are expressed as percentage of the maximal values obtained in the absence of FCCP.

not shown). In the presence of Mg^{2+}, post-State 3 respiration is limited by the rate of ATP cycling due to ATP hydrolysis by contaminating ATP hydrolases and by ATP synthesis by the mitochondrial F_1F_o ATP synthetase. Inhibition of the synthetase by the addition of oligomycin resulted in an additional shift toward reduction in the pyridine nucleotide redox state accompanied by a further stimulation of ROS generation. As expected, subsequent addition of the uncoupler FCCP resulted in maximal NAD(P)H oxidation and a decrease in ROS production to a level similar to that observed upon addition of ADP. Further verification that ROS generation is redox regulated came from the observation that subsequent addition of the Complex I inhibitor rotenone caused a maximal shift toward reduction of pyridine nucleotides and a maximal rate of H_2O_2 generation, even though $\Delta\Psi$ was already collapsed by the addition of FCCP.

The relationship between the rate of mitochondrial H_2O_2 production and NAD(P)H redox state was assessed by performing measurements of NAD(P)H autofluorescence in parallel to those of $\Delta\Psi$ described in Fig. 1. Thus the addition of increasing concentrations of the respiratory uncoupler FCCP was accompanied by increased NAD(P)H oxidation, consistent with greater membrane depolarization and accelerated respiration. As Fig. 3(a) demonstrates, FCCP-induced NAD(P)H oxidation is directly related to inhibition of H_2O_2 production. NAD(P)H oxidation is very sensitive to membrane depolarization, as shown in Fig. 3(b) where a 10% reduction in $\Delta\Psi$ is accompanied by an approximately 50% reduction in NAD(P)H fluorescence.

Discussion

The results of this study demonstrate that ROS production by isolated rat brain mitochondria respiring on NADH-dependent substrates is highly dependent on both mitochondrial membrane potential and NAD(P)H redox state. Moreover, this relationship is observed over a range of conditions that are consistent with those associated with normal fluctuations in cellular energy metabolism. Therefore, the rate of physiologically relevant mitochondrial ROS production can vary by several hundred percent, depending on whether energy demand is maximal (State 3 respiration) or ATP hydrolysis is minimal (State 4 respiration) (Fig. 1).

Relatively few measurements of mitochondrial ROS generation in the presence of NADH-linked respiratory substrates and in the absence of respiratory chain inhibitors have been reported, due to the low sensitivity of H_2O_2-sensitive indicators that were previously available. The utilization of Amplex Red enables detection of H_2O_2 at levels previously not considered significant (Starkov *et al.* 2002). The enhanced sensitivity of Amplex Red is also likely to be the explanation for why similar measurements using the fluorescent indicator scopoletin did not detect a relationship between $\Delta\Psi$ and H_2O_2 production in the presence of NADH-linked substrates (Votyakova and Reynolds 2001).

Mitochondrial ROS production is particularly sensitive to changes in $\Delta\Psi$ at the highest range of values (i.e. 170–185 mV) (Fig. 1). Quantification of this relationship can therefore only be accomplished with isolated mitochondria that are extremely well coupled and thus able to establish such high membrane potentials. We determined that including bovine serum albumin and EGTA in the incubation media helps mitochondria maintain high membrane potentials. Bovine serum albumin binds free fatty acids that can be generated from membrane lipids and that can uncouple mitochondria (Skulachev 1991). The Ca^{2+} chelator EGTA protects against any form of Ca^{2+}-induced mitochondrial dysfunction, including the membrane permeability transition that by definition results in uncoupling and membrane depolarization.

Although the relationship between $\Delta\Psi$, NAD(P)H redox state, and mitochondrial ROS production is apparent when these parameters are varied by the addition of either FCCP or ADP, the quantitative relationships are not identical. Thus,

the rates of ROS production with either saturating FCCP or ADP were approximately equal, but $\Delta\Psi$ was at least 20 mV higher with ADP (Fig. 1). Moreover, the NAD(P)H redox state was not as oxidized in the presence of ADP as it was in the presence of FCCP (Fig. 2). This apparent discrepancy may simply be due to a lack of control over ROS production at membrane potentials and pyridine nucleotide redox state at or below that maintained under State 3 respiration. Alternatively, differences in conditions present in the mitochondrial matrix during State 3 compared to uncoupled respiration might influence the site or sites responsible for ROS production. Additional evidence for the existence of membrane potential- and NAD(P)H/NAD(P)-independent ROS generation comes from the observation that the rate of H_2O_2 formation in the presence of rotenone was considerably greater than that observed in the presence of the ATP synthetase inhibitor oligomycin, even though the NAD(P)H autofluorescence was identical (Fig. 2). This difference could be due to a direct induction of ROS production by rotenone at Complex I in addition to its ability to induce a reduced shift in NAD(P)H and other redox sites proximal to the site at which rotenone inhibits electron transport (Ramsay and Singer 1992).

The site and the mechanism of ROS production by mitochondria oxidizing NADH-linked substrates in the absence of electron chain inhibitors are not fully characterized. Two fundamentally different mechanisms of ROS generation are possible. One mechanism involves the metabolism of NADH-dependent substrates to succinate and subsequent ROS production due to succinate oxidation by Complex II, and reversed electron flow through Complex I. The other mechanism is direct flow of electrons from NADH-dependent substrates to O_2 via one or more redox centers present within Complex I. In either case, the site of ROS generation within Complex I appears to be an iron-sulfur center within either the N2 or N1-a proteins (Genova *et al*. 2001; Kushnareva *et al*. 2002).

Dehydrogenases present in the mitochondrial matrix are functionally organized within the tricarboxylic acid cycle pathway and, with the aid of transaminases, allow for rapid interconversion of metabolic intermediates. Thus, metabolism of NADH-linked substrates can result in the formation of any TCA cycle intermediate, including (Von Korff *et al*. 1971; Von Korff and Kerpel-Fronius 1975; Beck *et al*. 1977; Kerpel-Fronius *et al*. 1977). Succinate oxidation stimulates ROS production at one or more sites located in Complex I via reverse electron transfer from Complex II through ubiquinone (Turrens 1997). Reversed electron transport is endergonic but can be driven by the energy present within a high membrane potential, as indicated by the complete inhibition of this process in the presence of uncouplers (Hansford *et al*. 1997; Korshunov *et al*. 1997; Votyakova and Reynolds 2001; Liu *et al*. 2002). The dependence of ROS production on $\Delta\Psi$ described in Fig. 1 might therefore be the consequence of metabolism to succinate and reversed electron flow to Complex I.

An alternative mechanism of ROS generation at Complex I specifically involves the redox state of NAD(P)H (Hansford *et al*. 1997*)*. Thus $\Delta\Psi$ may not affect ROS production directly but could regulate the rate of production through the close relationship between $\Delta\Psi$ and NAD(P)H redox state (Fig. 3). We propose that the ROS-producing site of Complex I is in redox equilibrium with mitochondrial pyridine nucleotides so that its degree of reduction depends on the $NADH/NAD^+$ ratio. This hypothesis is supported by the relationship between the rate of H_2O_2 production and the level of reduced pyridine nucleotides (Fig. 3), as has recently been described by Kushnareva *et al*. (2002). Additional evidence in support of this mechanism comes from the observation that superoxide production by rotenone-inhibited Complex I in submitochondrial particles also depends on the $NADH/NAD^+$ ratio and apparently originates from enzyme-bound reduced NADH (Krishnamoorthy and Hinkle 1988).

Although succinate-driven ROS production at Complex I is completely abolished by uncoupler-induced mitochondrial membrane depolarization (Hansford *et al*. 1997), we found that a significant fraction (30%) of H_2O_2 formation in the presence of NADH-linked substrates persists following maximal uncoupling (Fig. 1) and maximal NAD(P)H oxidation (Fig. 3). This observation supports the opinion that NADH-linked substrate-dependent ROS production is not indirectly due to succinate oxidation. The exact nature of this $\Delta\Psi$-independent ROS generation is unknown. However, preliminary results obtained with mitochondria and with isolated enzymes suggest that it could be mediated by the direct formation of superoxide by specific dehydrogenases, e.g. α-ketoglutarate dehydrogenase, and may be independent of Complex I mediated ROS production.

In conclusion, the results of this study emphasize the important role of ROS production by NADH-linked respiratory substrates in mitochondrial ROS generation. Mitochondrial ROS production in the presence of the Complex II substrate succinate is approximately 10 times greater than that of NADH-linked substrates at 5–10 mM substrate concentrations (Hansford *et al*. 1997; Korshunov *et al*. 1997; Votyakova and Reynolds 2001). Others have reported values for succinate-dependent ROS production that are comparable to the values we obtained for NADH-dependent generation (Barja and Herrero 1998; Herrero and Barja 1998). However, since succinate-dependent ROS generation is even more sensitive to a decline in $\Delta\Psi$ than is NADH-dependent ROS generation, variability among laboratories can be due to differences in $\Delta\Psi$ caused by different mitochondrial isolation procedures or incubation conditions. Although tissue succinate levels are normally much lower than the total concentration of NADH-linked respiratory substrates, concentrations of succinate do reach mM levels in

the brain and other tissues after periods of severe hypoxia induced by ischemia (Hoyer and Krier 1986; Camici *et al*. 1991). The redox state of pyridine nucleotides also shifts to a hyperoxidized level for up to 1 h during reperfusion following cerebral ischemia (Rosenthal *et al*. 1995). These conditions might allow for succinate-driven generation of ROS production at Complex I via reversed electron flow from Complex II (succinate dehydrogenase) and coenyzme Q. However, under normal conditions or when Complex I is inhibited by neurotoxins, e.g. MPP^+ or rotenone, ROS production at this site is far more likely to be fueled by the oxidation of NADH-dependent respiratory substrates (Sanchez-Ramos *et al*. 1988). We have now shown that NADH-dependent ROS generation is significant and regulated by physiological fluctuations in mitochondrial $\Delta\Psi$ and redox state. This finding provides further support for exploring neuroprotective interventions based on reducing mitochondrial ROS generation through limited respiratory uncoupling (Kim-Han *et al*. 2001; Ferranti *et al*. 2003).

Acknowledgements

This work was supported by USAMRMC Neurotoxin Initiative (DAMD 17-99-1-9483), NIH NS34152 and ES11838.

References

Barja G. and Herrero A. (1998) Localization at complex I and mechanism of the higher free radical production of brain nonsynaptic mitochondria in the short-lived rat than in the longevous pigeon. *J. Bioenerg. Biomembr.* **30**, 235–243.

Beck D. P., Broyles J. L. and Von Korff R. W. (1977) Role of malate transport in regulating metabolism in mitochondria isolated from rabbit brain. *J. Neurochem.* **29**, 487–493.

Camici P., Marraccini P., Lorenzoni R., Ferrannini E., Buzzigoli G., Marzilli M. and L'Abbate A. (1991) Metabolic markers of stress-induced myocardial ischemia. *Circulation* **83**, III8–13.

Echtay K. S. *et al.* (2002) Superoxide activates mitochondrial uncoupling proteins. *Nature* **415**, 96–99.

Ferranti R., da Silva M. M. and Kowaltowski A. J. (2003) Mitochondrial ATP-sensitive K^+ channel opening decreases reactive oxygen species generation. *FEBS Lett.* **536**, 51–55.

Fiskum G. (2000) Mitochondrial participation in ischemic and traumatic neural cell death. *J. Neurotrauma* **17**, 843–855.

Genova M. L., Ventura B., Giuliano G., Bovina C., Formiggini G., Parenti C. G. and Lenaz G. (2001) The site of production of superoxide radical in mitochondrial Complex I is not a bound ubisemiquinone but presumably iron-sulfur cluster N2. *FEBS Lett.* **505**, 364–368.

Hansford R. G., Hogue B. A. and Mildaziene V. (1997) Dependence of H_2O_2 formation by rat heart mitochondria on substrate availability and donor age. *J. Bioenerg. Biomembr.* **29**, 89–95.

Hashimoto K., Angiolillo P. and Rottenberg H. (1984) Membrane potential and surface potential in mitochondria. Binding of a cationic spin probe. *Biochim. Biophys. Acta* **764**, 55–62.

Herrero A. and Barja G. (1998) H_2O_2 production of heart mitochondria and aging rate are slower in canaries and parakeets than in mice: sites of free radical generation and mechanisms involved. *Mech. Ageing Dev.* **103**, 133–146.

Hoyer S. and Krier C. (1986) Ischemia and aging brain. Studies on glucose and energy metabolism in rat cerebral cortex. *Neurobiol. Aging* **7**, 23–29.

Kamo N., Muratsugu M., Hongoh R. and Kobatake Y. (1979) Membrane potential of mitochondria measured with an electrode sensitive to tetraphenyl phosphonium and relationship between proton electrochemical potential and phosphorylation potential in steady state. *J. Membr. Biol.* **49**, 105–121.

Kerpel-Fronius S., Beck D. P. and Von Korff R. W. (1977) Studies on the metabolism of glutamate and glutamine by mitochondria from rabbit brain: complications due to isotopic exchange reactions. *J. Neurochem.* **28**, 871–875.

Kim-Han J. S., Reichert S. A., Quick K. L. and Dugan L. L. (2001) BMCP1: a mitochondrial uncoupling protein in neurons which regulates mitochondrial function and oxidant production. *J. Neurochem.* **79**, 658–668.

Korshunov S. S., Skulachev V. P. and Starkov A. A. (1997) High protonic potential actuates a mechanism of production of reactive oxygen species in mitochondria. *FEBS Lett.* **416**, 15–18.

Krishnamoorthy G. and Hinkle P. C. (1988) Studies on the electron transfer pathway, topography of iron-sulfur centers, and site of coupling in NADH-Q oxidoreductase. *J. Biol. Chem.* **263**, 17566–17575.

Kushnareva Y. E., Murphy A. N. and Andreyev A. Y. (2002) Complex I mediated reactive oxygen species generation: Modulation by Cytochrome *c* and NAD(P)+ oxidation-reduction state. *Biochem. J.* **368**, 545–553.

Liu Y., Fiskum G. and Schubert D. (2002) Generation of reactive oxygen species by the mitochondrial electron transport chain. *J. Neurochem.* **80**, 780–787.

Nicholls D. G. and Budd S. L. (2000) Mitochondria and neuronal survival. *Physiol. Rev.* **80**, 315–360.

Ramsay R. R. and Singer T. P. (1992) Relation of superoxide generation and lipid peroxidation to the inhibition of NADH-Q oxidoreductase by rotenone, piericidin A, and MPP+. *Biochem. Biophys. Res. Commun* **189**, 47–52.

Rolfe D. F., Hulbert A. J. and Brand M. D. (1994) Characteristics of mitochondrial proton leak and control of oxidative phosphorylation in the major oxygen-consuming tissues of the rat. *Biochim. Biophys. Acta* **1188**, 405–416.

Rosen G. M., Tsai P., Weaver J. M., Porasuphatana S., Roman L. J., Starkov A. A., Fiskum G. and Pou S. (2002) Tetrahydrobiopterin: Its role in the regulation of neuronal nitric oxide synthase-generated superoxide. *J. Biol. Chem.* **277**, 40275–40280.

Rosenthal R. E., Hamud F., Fiskum G., Varghese P. J. and Sharpe S. (1987) Cerebral ischemia and reperfusion: prevention of brain mitochondrial injury by lidoflazine. *J. Cereb. Blood Flow Metab.* **7**, 752–758.

Rosenthal M., Feng Z. C., Raffin C. N., Harrison M. and Sick T. J. (1995) Mitochondrial hyperoxidation signals residual intracellular dysfunction after global ischemia in rat neocortex. *J. Cereb. Blood Flow Metab.* **15**, 655–665.

Rottenberg H. (1984) Membrane potential and surface potential in mitochondria: uptake and binding of lipophilic cations. *J. Membr. Biol.* **81**, 127–138.

Sanchez-Ramos J. R., Hollinden G. E., Sick T. J. and Rosenthal M. (1988) 1-Methyl-4-phenylpyridinium (MPP+) increases oxidation of cytochrome-*b* in rat striatal slices. *Brain Res.* **443**, 183–189.

Sherer T. B., Betarbet R. and Greenamyre J. T. (2002) Environment, mitochondria, and Parkinson's disease. *Neuroscientist* **8**, 192–197.

Skulachev V. P. (1991) Fatty acid circuit as a physiological mechanism of uncoupling of oxidative phosphorylation. *FEBS Lett.* **294**, 158–162.

Starkov A. A., Polster B. M. and Fiskum G. (2002) Regulation of hydrogen peroxide production by brain mitochondria by calcium and Bax. *J. Neurochem.* **83**, 220–228.

Turrens J. F. (1997) Superoxide production by the mitochondrial respiratory chain. *Biosci. Rep.* **17**, 3–8.

Von Korff R. W. and Kerpel-Fronius S. (1975) The effect of cosubstrates on tricarboxylic acid cycle dynamics during pyruvate oxidation: the formation of alpha-ketoglutarate and utilization of glutamate by mitochondria from rabbit brain. *J. Neurochem.* **25**, 767–778.

Von Korff R. W., Steinman S. and Welch A. S. (1971) Metabolic characteristics of mitochondria isolated from rabbit brain. *J. Neurochem.* **18**, 1577–1587.

Votyakova T. V. and Reynolds I. J. (2001) DeltaPsi(m)-Dependent and -independent production of reactive oxygen species by rat brain mitochondria. *J. Neurochem.* **79**, 266–277.